Investigation of the Role of the N-Terminal Proline, the Distal Heme Ligand in the CO Sensor CooA†

Robert W. Clark,‡ Hwan Youn,§ Ryan B. Parks,‡ Melisa M. Cherney,‡ Gary P. Roberts,§ and Judith N. Burstyn*,‡

Departments of Chemistry and Bacteriology, University of Wisconsin, Madison, Wisconsin 53706

Received June 9, 2004; Revised Manuscript Received August 18, 2004

ABSTRACT: A unique feature of CooA, a heme-containing transcription factor, is that the N-terminal proline is the distal heme ligand in the ferrous state, and this ligand is displaced upon CO binding. To investigate the importance of Pro^2 in CO-dependent DNA binding, several CooA variants that alter N-terminal ligation were characterized. Electronic absorption, electron paramagnetic resonance, and magnetic circular dichroism spectra of these variants provide the most definitive evidence that Pro^2 is the distal ligand in Fe(III) CooA. Furthermore, the functional and spectroscopic properties of these proteins depended on whether a weak ligand occupied the distal heme coordination site: for CooA variants in which distal coordination is disrupted, the DNA-binding affinities and Fe(II)−CO spectral properties showed an unexpected dependence on the order of CO addition and heme reduction. If N-terminal variant samples were incubated with CO before the heme was reduced, the proteins displayed DNA-binding affinities and Fe(II)−CO spectral characteristics similar to those of wild-type (WT) CooA. However, if the same samples were incubated with CO after the heme was reduced, the extent of functional and spectral similarity to WT CooA negatively correlated with the amount of high-spin heme present in the ferric state. From these data, it was inferred that the absence of a distal heme ligand in the ferric state prevents WT-like CO binding to the ferrous state, and it was hypothesized that correct CO binding is inhibited by the collapse of the distal heme pocket upon reduction. Together with the observation that L116H CooA, a variant in which His^{116} replaces Pro^2 as the distal heme ligand, binds CO more slowly than WT CooA, these data indicate that the presence of a weak distal heme ligand, not specifically ligation by the N-terminal proline, is crucial for proper function. The role of Pro^2 in CooA is apparently to direct CO to bind on the distal side of heme and to help maintain the integrity of the distal heme pocket during the redox-mediated ligand switch.

Numerous essential physiological functions are regulated by proteins that have evolved to sense small gas molecules (*1*−*6*). In mammals, the sensing of nitric oxide by soluble guanylyl cyclase (sGC)[1] (*7*, *8*) results in the production of the second messenger cyclic guanosine monophosphate (cGMP), which is critical in smooth-muscle relaxation and vasodilation (*9*). In plant-associated rhizobia, the expression of genes involved in nitrogen fixation is regulated by FixL histidine kinase, which senses oxygen and shuts down its kinase activity in response (*10*, *11*). In *Rhodospirillum rubrum*, the recognition of CO by CooA (*12*, *13*), a transcription factor, allows *R. rubrum* to grow using CO as its sole energy source (*14*). A defining characteristic of gas-sensing proteins is that a metal cofactor typically serves as the effector recognition site; for proteins such as sGC, FixL, and CooA, the specific cofactor utilized is heme.

CooA is the first known CO-specific, gas-sensing heme protein (*13*, *15*). CooA is a homodimer containing one *b*-type heme in each 24.6 kDa monomer (*13*) and is a member of the cyclic adenosine monophosphate (cAMP) receptor protein (CRP) and fumarate and nitrate reductase protein superfamily of transcriptional regulators (*16*). Like other members of the CRP family, CooA is composed of two distinct domains: an effector-binding regulatory domain and a DNA-binding domain. In the presence of CO and anaerobic growth conditions, CooA binds to DNA and promotes the transcription of genes encoding a CO-oxidation system (*12*). The binding of CO to heme in the regulatory domain is proposed to trigger a global conformational change that correctly positions the DNA-recognition F-helices to bind DNA (*17*). A comparison of the crystal structures of the Fe(II) effector-free form of CooA with the DNA- and cAMP effector-bound form of CRP suggests that the signal may be propagated from the heme to the DNA-binding domain by repositioning the C-helices, the long α-helices that form a leucine zipper motif at the dimer interface (*18*). Mutagenesis studies, which investigated residues participating in the leucine zipper motif,

† This work was supported in part by NIH Grants GM-53228 (G.P.R.) and HL-66147 (J.N.B).

* Address correspondence to this author at the Department of Chemistry, University of Wisconsin−Madison, 1101 University Ave., Madison, WI 53706 [telephone (608) 262-0328; fax (608) 262-6143; e-mail burstyn@chem.wisc.edu].

‡ Department of Chemistry.

§ Department of Bacteriology.

[1] Abbreviations: cAMP, cyclic adenosine monophosphate; CAPS, 3-(cyclohexylamino)-1-propanesulfonic acid; CD, circular dichroism; cGMP, cyclic guanosine monophosphate; CHES, 2-(cyclohexylamino)-ethanesulfonic acid; CRP, cAMP receptor protein; EPR, electron paramagnetic resonance; LMCT, ligand-to-metal charge transfer; Mb, myoglobin; MCD, magnetic circular dichroism; MES, 2-(*N*-morpholino)ethanesulfonic acid; MOPS, 3-(*N*-morpholino)propanesulfonic acid; NMR, nuclear magnetic resonance; sGC, soluble guanylyl cyclase; WT, wild type.

10.1021/bi0487948 CCC: $27.50
Published on Web 10/08/2004

support a prominent role for the C-helices in signal transmission (*19*).

The heme of CooA exists in three distinguishable states: Fe(III), Fe(II), and Fe(II)−CO (*13*, *15*). In all of these forms, the heme is 6-coordinate and low-spin, implying that CO binding leads to the displacement of one heme ligand. In Fe(III) CooA, several spectroscopic and mutagenesis studies have conclusively shown that the proximal heme ligand is Cys^{75} (*17*, *20*−*22*). Definitive evidence identifying the distal ligand in the ferric state is not available, although available data support a neutral nitrogen donor occupying this coordination site. A 2.6 Å X-ray crystal structure of Fe(II) CooA confirmed that His^{77} replaces Cys^{75} as the proximal ligand upon reduction and also identified the N-terminal residue, Pro^2, as a novel heme ligand on the distal side (*18*). Remarkably, the N-terminal proline from one monomer of CooA is the ligand for the heme of the opposite monomer. Finally, for the Fe(II)−CO state, nuclear magnetic resonance (NMR) and mutagenesis studies have indicated that the addition of CO results in the displacement of Pro^2, whereas His^{77} remains coordinated to heme (*23*).

The identification of Pro^2 as the distal heme ligand in Fe(II) CooA was unexpected (*18*). CooA is the first protein found to utilize proline as a heme ligand and, along with cytochrome *f*, is only the second reported example in which the N-terminal amino group coordinates the heme (*24*). The electronic and structural properties of proline, a secondary amine, would seem to make it an unlikely heme ligand. The pK_a for deprotonation of free proline is 10.64 (*25*); thus, proline is expected to be fully protonated at physiological pH and unable to bind heme. Although the formation of a strong Fe−N bond coupled with a low local dielectric environment might be expected to lower the high pK_a of proline, repulsive steric interactions between the secondary amine and the porphyrin ring should significantly weaken Fe−N bonding interactions. Published crystal structures of iron porphyrin model complexes bearing secondary amine ligands support this explanation by displaying increased Fe−N−C bond angles or lengthened Fe−N bond distances, presumably to compensate for an unfavorable steric interaction between the amine and the porphyrin (*26*−*28*). The presence of the unusual Pro^2 ligand in CooA suggests this residue may serve an important function in CooA activation.

Initial studies that investigated the role of the N-terminal proline suggested that Pro^2 is not essential for CO-dependent DNA binding (*29*, *30*). Mutagenesis of N-terminal residues 2−6 revealed that a wide variety of protein variants with altered N-terminal sequences displayed CO-responsive activity in vivo (*29*). One of these variants, P2Y, displayed CO-specific in vitro DNA binding similar to that of wild-type (WT) CooA, although its spectroscopic properties were modestly different from those of the native protein. Surprisingly, these results seem to imply that Pro^2 is not essential for CO-dependent DNA binding in CooA, despite the unprecedented discovery of Pro^2 as a heme ligand. In the current study, we have characterized a series of purified CooA variants that change the length and identity of the N terminus (subsequently referred to as the N-terminal variants) in order to further explore the role of Pro^2 in the structure and function of CooA (Table 1). In this paper, we provide evidence that Pro^2 is the distal ligand in the Fe(III) state and demonstrate that Pro^2 is important for CooA function because of its relatively weak ligation to the heme.

Table 1: Properties of CooA Variants with Alterations to the Distal Heme Environment

variant	N-terminal sequence	N-terminal length[a]	retains Met[1]
WT	PPRFN	WT	no
P2V[b]	VPRFN	WT	no
P2H[b]	MHPRFN	+1 aa	yes
P2Y[c]	MYPRFN	+1 aa	yes
ΔP3R4[b]	PFN	−2 aa	no

[a] Relative number of N-terminal residues compared to WT CooA. [b] Molecular mass determined by electrospray ionization mass spectrometry is in agreement with the calculated value. [c] The N-terminal sequence of this variant was previously verified (*29*).

EXPERIMENTAL PROCEDURES

Expression and Purification of WT CooA and CooA Variants. WT CooA and CooA variants were constructed in an *Escherichia coli* overexpression system as previously described (*17*). WT CooA and the N-terminal CooA variant proteins were purified to >90% purity using the protocol previously reported (*17*). L116H CooA was purified to ∼85% purity in the same manner used to purify L116K CooA (*31*). The heme content of CooA preparations was measured using the reduced pyridine−hemochromogen method (*32*). Electrospray ionization mass spectrometry was used to verify the predicted molecular masses of P2V, P2H, and ΔP3R4 CooA. The N-terminal sequence of P2Y CooA was determined previously (*29*).

Electron Absorption Spectroscopy. Electronic absorption spectra were recorded at room temperature on a Varian Cary 4 Bio spectrophotometer set to a spectral bandwidth of 0.5 nm. Samples were prepared by diluting CooA stock solutions into degassed solutions of 25 mM sodium citrate (pH 3.0), 25 mM 3-(*N*-morpholino)propanesulfonic acid (MOPS) (pH 7.5), or 25 mM 3-(cyclohexylamino)-1-propanesulfonic acid (CAPS) (pH 10.0) buffer. All buffers contained 0.1 M NaCl except for the 25 mM MOPS solution used for L116H, which required 0.5 M NaCl for protein stability. The Fe(III) samples were prepared by diluting the as-isolated proteins into the appropriate buffer solution to obtain a final concentration of 5−10 μM heme. The Fe(II) samples were prepared by adding a sodium dithionite solution (2 mM final concentration) to an Ar-purged vial containing degassed Fe(III) CooA. The Fe(II)−CO CooA samples were prepared either by (1) injecting 800−1000 μL of CO gas into the headspace of vials containing Fe(II) CooA and mixing the CO gas by gentle rocking, (2) adding 800−1000 μL of CO gas into the headspace of Ar-purged vials containing degassed Fe(III) CooA, mixing the CO gas by gentle rocking, and subsequently adding a sodium dithionite solution (2 mM final concentration), or (3) adding CO-saturated buffer (∼100 μM final concentration) and 500 μL of CO gas into the headspace of sealed vials containing Fe(II) CooA and mixing the CO solution by gentle rocking (L116H). For Fe(II)−CO L116H, spectra were recorded at multiple time points over the course of ∼8 h.

Electronic Paramagnetic Resonance (EPR) Spectroscopy. EPR spectra were recorded on a Bruker ESP 300E spectrometer equipped with an Oxford ESR 900 continuous flow cryostat and an Oxford ITC4 temperature system to monitor

and regulate the temperature. The microwave frequency was monitored using a Varian EIP model 625A CW frequency counter. The field was calibrated with a Bruker 035 M gaussmeter. Fe(III) CooA EPR samples were prepared in 100 mM sodium acetate (pH 4.0), 100 mM MOPS (pH 7.4), or 100 mM CAPS (pH 10.0) buffer. All buffers contained 0.1 M NaCl except where noted in the text. Final heme concentrations are 50 μM unless otherwise noted. EPR samples were prepared under an argon atmosphere and were frozen and stored in liquid nitrogen. Except where noted, the EPR spectra were recorded at X-band and 10 K; each reported spectrum is composed of 1024 points. Specific conditions for the recording of each spectrum are given in the figure legends.

Magnetic Circular Dichroism (MCD) Spectroscopy. MCD spectra were recorded on a Jasco J-715 circular dichroism (CD) spectropolarimeter modified to accommodate an SM-4000 8 T magnetocryostat (Oxford Instruments). Each spectrum represents the average of at least three accumulations taken at a resolution of 1 nm and a scan speed of 200 nm/min. The instrument bandwidth was 2 nm with a response time of 0.25 s. All MCD spectra were taken at 7 T and at multiple temperatures ranging from 4.5 to 100 K as appropriate. Natural CD was subtracted from the MCD spectrum for all samples. Samples were prepared by diluting protein stock solutions into 125 mM 2-(*N*-morpholino)-ethanesulfonic acid (MES) (pH 6.5), 125 mM MOPS (pH 7.5), or 125 mM 2-(cyclohexylamino)ethanesulfonic acid (CHES) (pH 9.5) buffer. Glycerol [55% (v/v)] was used as a glassing agent. Reduced and carbonylated samples were prepared analogously to samples prepared for electronic absorption spectroscopy and were frozen and stored in liquid nitrogen. Final heme concentrations were 50 μM unless otherwise noted.

Fluorescence Polarization Assays. In vitro DNA-binding assays were performed using a fluorescence polarization method (*29*). Target duplex DNA, which contained pCooF and was labeled with the fluorescent dye Texas Red on the 5′ end of one oligonucleotide, was purchased from Genosys and used at a concentration of 6.4 nM. Dissociation constants (K_d) were calculated by fitting the binding data to a nonlinear equation as previously described (*33*).

RESULTS

Altering the Length and Identity of the N-Terminal Residues Results in a Mixture of 5-Coordinate, High-Spin and 6-Coordinate, Low-Spin Heme in the Fe(III) N-Terminal CooA Variants. Spectroscopic characterization of the N-terminal CooA variants indicates that changes to the N-terminal sequence significantly alter the heme environment in the ferric state. We studied a series of CooA variants, denoted P2V, P2H, P2Y, and ΔP3R4, with varied N-terminal lengths, different N-terminal residues, and good stability upon purification (Table 1). The N-terminal residue Met^1 is proteolytically cleaved in vivo for proteins in which the second residue is small; therefore, Pro^2 is the N terminus for WT CooA, and Val^2 is the N terminus for P2V. In contrast, P2H and P2Y have large amino acid substitutions; therefore, Met^1 is retained as the N-terminal residue in these variants. Finally, ΔP3R4, which lacks Pro^3 and Arg^4, retains Pro^2 as the N terminus but is two residues shorter than WT CooA.

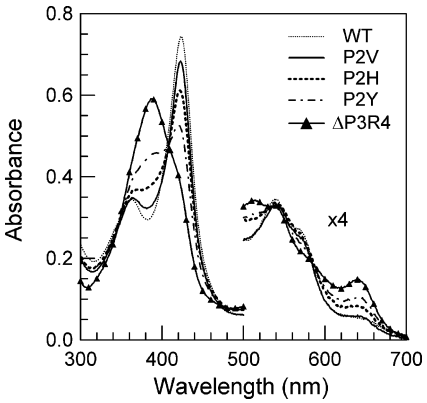

FIGURE 1: Alteration of the N terminus of Fe(III) CooA perturbs heme coordination. Electronic absorption spectra of the ferric forms of WT, P2V, P2H, P2Y, and ΔP3R4 CooA are shown. The samples were ~7.5 μM in heme and were prepared in 25 mM MOPS (pH 7.5) containing 0.1 M NaCl.

Electronic absorption spectra suggest that the Fe(III) forms of P2H, P2Y, and ΔP3R4 have significantly disrupted heme environments containing mixed populations of two coordination states at physiological pH, whereas Fe(III) P2V is predominantly 6-coordinate, low-spin, and has a heme environment similar to that of native CooA (Figure 1). Although the electronic absorption spectrum of Fe(III) WT CooA exhibited a unique Soret peak at 424 nm, spectra of CooA variants possessing N termini of lengths differing from that of WT CooA (P2H, P2Y, and ΔP3R4) displayed two distinct Soret bands centered near 385 and 424 nm (Figure 1; Table S1, Supporting Information). Spectra of these N-terminal variants also contained extra α and β features from 500 to 600 nm, unlike WT CooA, which had only two peaks at 539 (β) and 573 (α) nm. Finally, the intensity of the thiolate sulfur-to-Fe(III) charge-transfer transition at 641 nm increased as the N-terminal length of the variants deviated from that of WT CooA. The positions and intensities of the multiple Soret, α, β, and ligand-to-metal charge transfer (LMCT) absorption bands are consistent with a mixture of 5-coordinate, high-spin, and 6-coordinate, low-spin, cysteine thiolate-bound heme (Table S1, Supporting Information) (*34*−*39*). In contrast, the absorption spectrum of Fe(III) P2V, which has an N terminus the same length as the native protein, was closest to that of Fe(III) WT CooA among the N-terminal variants. Specifically, the optical spectrum of Fe(III) P2V contained only one distinct set of Soret, α, and β features that occurred at virtually identical positions to those of WT CooA (Figure 1; Table S1, Supporting Information).

The relative intensities of the two major Soret features in the N-terminal variant spectra vary with pH and N-terminal length. Overlaid spectra of the N-terminal variants displayed isosbestic-like behavior with a crossing point at 408 nm (Figure 1). Similar interconversion between the two major components was observed in all variants as a function of pH (Figure S1, Supporting Information). Electronic absorption spectra of the N-terminal variants at pH 3.0 displayed only one Soret feature near 385 nm, indicative of an exclusively high-spin heme, whereas absorption spectra of the variants at pH 10.0 displayed a major Soret feature near 424 nm, indicative of a greater proportion of 6-coordinate, low-spin heme. At pH 10.0, P2V and P2H appeared to be predominately 6-coordinate, whereas P2Y and ΔP3R4 still

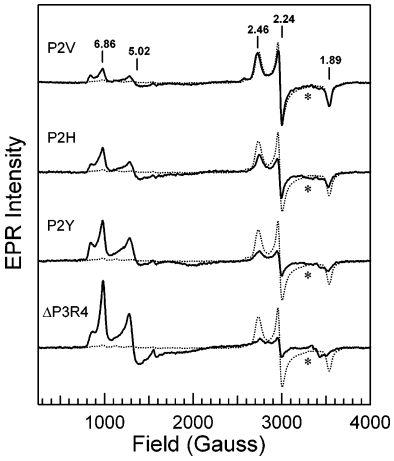

FIGURE 2: N-Terminal CooA variants contain a mixture of $S = {}^1/_2$ and $S = {}^5/_2$ heme at physiological pH. EPR samples were prepared in 100 mM MOPS (pH 7.4) containing 0.1 M NaCl. All spectra represent the average of 16 scans and were taken at 10 K with a ~9.36-GHz microwave frequency, 100-kHz modulation frequency, and 8.3-G modulation amplitude. The spectra of P2V, P2H, P2Y, and ΔP3R4 CooA (solid lines), 50 μM in heme, were recorded at 1.011 mW of microwave power with a 1.0×10^6 receiver gain. The spectrum of WT CooA (dotted line), 105 μM in heme, was recorded at 0.505 mW of microwave power with a 6.3×10^5 receiver gain. The EPR spectrum of WT has been appropriately scaled to accurately compare peak intensities to spectra of the N-terminal variants. The asterisk denotes a signal present in the cavity.

contained a significant amount of high-spin heme, evident by a Soret feature near 385 nm. This isosbestic-like behavior suggests that the deprotonation/protonation of a common (or similar) ligand is responsible for the two heme coordination states observed in the variant proteins. Notably, the relative intensities of the high- and low-spin features and their pH-dependent interconversion appear to relate to the length of the N terminus. Fe(III) P2V, with an N terminus the same length as that of WT CooA, contained the least high-spin heme, whereas Fe(III) ΔP3R4, with the shortest N terminus, contained the most high-spin heme. Fe(III) P2H and Fe(III) P2Y, proteins with N termini that are one amino acid longer than WT CooA, differed from one another, with Fe(III) P2H having a noticeably larger amount of low-spin heme than Fe(III) P2Y. This difference may be attributable to a subpopulation of P2H in which His^2 serves as the distal heme ligand (vide infra).

EPR spectra of the N-terminal variants reveal a mixture of $S = {}^1/_2$ and $S = {}^5/_2$ hemes, the composition of which varies with pH and with N-terminal length, confirming spin-state assignments made using electronic absorption spectroscopy. All of the N-terminal variants contained at least one set of rhombic signals at high field (2000−4000 G), similar to those of WT CooA and indicative of low-spin ($S = {}^1/_2$) heme (Figure 2). The g anisotropies of the $S = {}^1/_2$ signals were characteristic of a cysteine-ligated, 6-coordinate heme (Table S2, Supporting Information) (*21*, *36*, *40*−*43*); the rhombicity and tetragonality parameters placed these features in the P region of a Blumberg−Peisach plot (*44*). At low field (500−2000 G), EPR spectra of the N-terminal variants also contained at least two sets of signals that are indicative of high-spin ($S = {}^5/_2$) heme. The positions of both sets of $S = {}^5/_2$ signals are most consistent with cysteine-ligated, 5-coordinate heme (Table S2, Supporting Information) (*36*, *40*, *45*−*48*). The presence of a major and a minor set of $S = {}^5/_2$ rhombic signals was previously noted in EPR studies of Fe(III) P2Y CooA, although the origin of the multiple sets of signals is not clear (*29*). Consistent with results obtained by electronic absorption spectroscopy, the ratio of $S = {}^1/_2$ signals to $S = {}^5/_2$ signals varied with both pH (data not shown) and N-terminal length (Figure 2). Variants having N termini that differed most from that of WT CooA showed the greatest pH-dependent changes in their spectra.

The positions and intensities of the $S = {}^1/_2$ signals in EPR spectra of the N-terminal variants suggest that the distal heme ligand in these proteins is a weak nitrogen donor (Figure 2; Table S2, Supporting Information) (*21*, *36*, *40*−*43*). In particular, the g_z feature between 2720 and 2750 G (g_z = 2.43−2.46) occurred at a position typical for thiolate-ligated complexes bearing O-atom donors or weak N-atom donors, but fell outside the usual range for complexes bearing a strong trans ligand such as histidine. Moreover, the g_z signals were sharper and noticeably more intense than the same features observed for heme complexes bearing distal O-atom donor ligands, suggesting that the distal ligand is not oxygen-based. Rather, the combined positions and intensities of the g_z signals in the variant spectra are most like those of cytochrome P450 complexes bearing weak nitrogen-donor ligands, implying that the N-terminal variants may have similar distal ligands (Table S2, Supporting Information) (*41*). A possible donor ligand with these properties in the variant proteins is the N-terminal amino group. The major g_z signal observed in the EPR spectrum of Fe(III) WT CooA is similar to that of the N-terminal variants, suggesting that native CooA and the N-terminal variants all utilize a weak nitrogen-donor ligand (Figure 2; Table S2, Supporting Information) (*21*).

MCD spectroscopy provides conclusive evidence that the high-spin ($S = {}^5/_2$) Fe(III) heme in the N-terminal CooA variants is 5-coordinate. Both high- and low-spin 6-coordinate hemes display intense positive and negative temperature-dependent *C* terms in the Soret region of the MCD spectrum (commonly referred to as pseudo *A* terms); 5-coordinate, high-spin hemes bearing either nitrogen or sulfur ligands display only weak negative *C* terms in this region (*36*, *49*−*52*). MCD spectra of the N-terminal CooA variants contained features arising from a mixture of 5- and 6-coordinate hemes (Figure 3). Spectra of both WT CooA and the N-terminal variants exhibited a derivative-shaped pseudo *A* term centered near 420 nm; however, spectra of the variant proteins also exhibited an additional negative band at 393 nm in the Soret region. The feature at 393 nm in the variant spectra is indicative of 5-coordinate, $S = {}^5/_2$, heme and occurs at a position typical for 5-coordinate heme proteins bearing a proximal cysteine ligand (*36*, *49*−*51*). To verify this assignment, the MCD spectrum of G117I CooA, a known 5-coordinate cysteine-ligated CooA variant, was also acquired (Figure S2, Supporting Information). Key features in the Fe(III) G117I MCD spectrum include negative terms at 393 and 547 nm and a positive term at 636 nm (Figure S2, Supporting Information), all of which displayed the characteristic temperature-dependent behavior of *C* terms (data not shown). Identical bands were observed in the spectra of the Fe(III) forms of P2H, P2Y, and ΔP3R4; however, these bands were substantially less intense or absent in spectra of

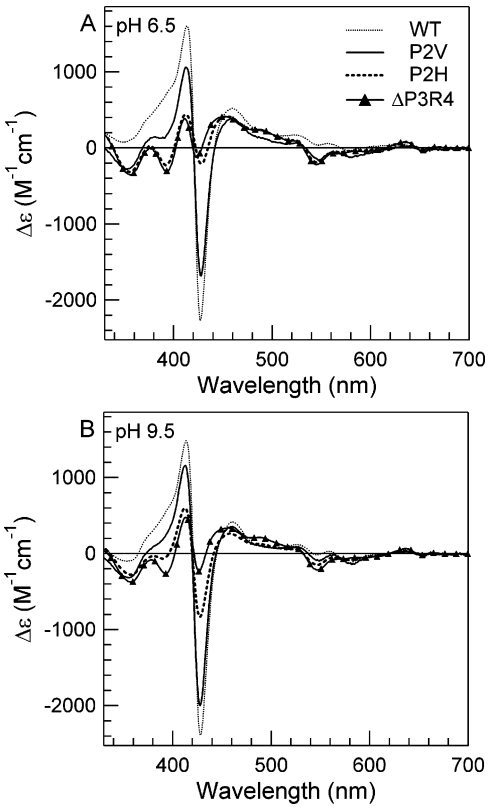

FIGURE 3: MCD spectroscopy reveals that the Fe(III) N-terminal variants possess a mixture of 5- and 6-coordinate heme. MCD samples were either 30 μM (P2V) or 50 μM (WT, P2H, and ΔP3R4) in heme and were prepared in 125 mM MES (pH 6.5) (A) or 125 CHES mM pH 9.5 (B) with 55% (v/v) glycerol. All MCD spectra shown were taken at a temperature of 25.0 K in a field of 7 T. The MCD spectra of P2V were scaled by $^5/_3$ for comparison. The MCD spectra of P2Y displayed mixed heme coordination similar to that of P2H and were omitted for clarity.

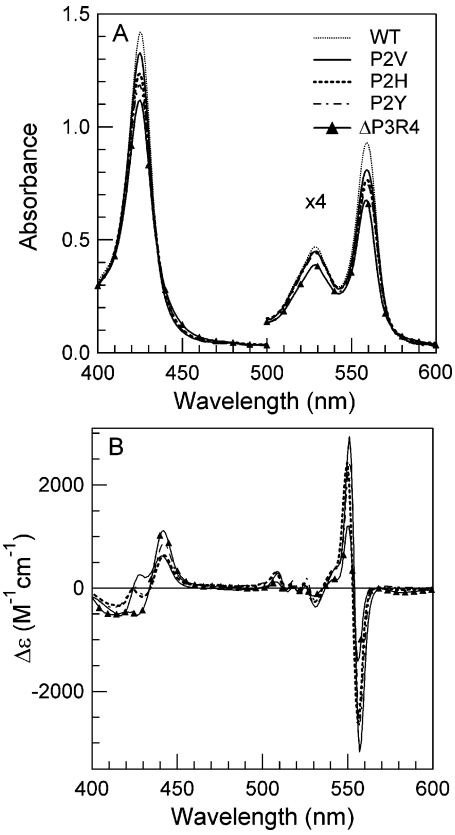

FIGURE 4: Electronic absorption (A) and MCD spectra (B) of the Fe(II) N-terminal variants reveal mixed coordination in the reduced state. (A) The samples used for electronic absorption spectroscopy were 7.5 μM in heme and were prepared in 25 mM MOPS (pH 7.5) containing 0.1 M NaCl. Electronic absorption spectra were recorded at room temperature. (B) MCD samples were either 25 μM (P2V) or 50 μM (P2H, P2Y, and ΔP3R4) in heme and were prepared in 125 mM MOPS (pH 7.5) buffer with 55% (v/v) glycerol. All MCD spectra shown were recorded at a temperature of 4.5 K in a field of 7 T. The MCD spectrum of P2V was scaled by a factor of 2 for comparison. The MCD spectrum of Fe(II)WT was omitted for clarity, but has been previously reported and contains *A* terms centered at 420 and 554 nm (22).

P2V and WT CooA, respectively (Figure 3). The similarity of the high-spin MCD absorptions of Fe(III) P2H, Fe(III) P2Y, and Fe(III) ΔP3R4 to those of Fe(III) G117I confirms that these CooA variants contain significant amounts of 5-coordinate, cysteine-ligated, high-spin heme.

The relative intensities of the MCD features of the Fe(III) N-terminal CooA variants confirmed that the proportion of 5- and 6-coordinate hemes present varied with pH and the length of the N terminus. Analogous to electronic absorption and EPR studies presented above, variants having N termini that differed from that of WT CooA showed pH-dependent changes in their spectra (Figure 3). MCD spectra of variants such as P2H and P2Y prepared at pH 3.0 were characteristic of an exclusively 5-coordinate, cysteine-ligated, high-spin heme (data not shown).

Fe(II) N-Terminal CooA Variants Exhibit Spectral Properties Similar to Those of Fe(II) WT CooA but with a Fraction of High-Spin Heme. Electronic absorption spectra of the Fe(II) states suggest that the N-terminal CooA variants contain a significant proportion of 6-coordinate, low-spin heme at physiological pH. Peak positions of key bands in spectra of the N-terminal variants, such as the Soret (425 nm), β (528 nm), and α (559 nm) bands, occur at wavelengths virtually identical to those of Fe(II) WT CooA, which is fully 6-coordinate and low-spin (Figure 4A). All Fe(II) N-terminal variants also behave like Fe(II) WT CooA (Figure 4A), exhibiting an increased Soret extinction coefficient relative to the Soret band of the Fe(III) state (Figure 1). However, subtle differences in band shapes and intensities exist when the variant spectra are compared to each other and to that of Fe(II) WT CooA (Figure 4A). These spectral perturbations are consistent with the presence of some high-spin ferrous heme in the N-terminal variants.

MCD spectroscopy, which readily distinguishes between high- and low-spin Fe(II) hemes, reveals a mixture of high- and low-spin ferrous hemes in the N-terminal CooA variants. MCD spectra of the Fe(II) N-terminal CooA variants contain a mixture of both *A* terms and *C* terms. Because low-spin Fe(II) hemes have an $S = 0$ ground state and exhibit temperature-independent *A* terms, whereas high-spin Fe(II) hemes have an $S = 2$ ground state and exhibit temperature-dependent *C* terms, the presence of both types of signals implies a mixture of spin states in the variants. Characteristic low-spin spectral features, including the Soret- and α-band *A* terms at 420−423 and ∼554 nm, respectively, are observed in spectra of both the Fe(II) N-terminal variants (Figure 4B) and WT CooA (*22*), implying the low-spin hemes in all of these proteins have similar coordination structures. In the variants, temperature-dependent *C* terms, observed as a negative band near 428 nm and a positive band near 443

Table 2: Electronic Absorption Data and DNA Binding Affinities Observed for the CO-Bound CooA Variants, Which Were Formed by Adding the CO Effector either before or after Reduction of Heme[a]

	heme reduction → CO addition			CO addition → heme reduction			
variant	Soret (ϵ)[b]	A_β/A_α[c]	K_{d1}[d] (nM)	Soret (ϵ)[b]	A_β/A_α[c]	K_{d2}[d] (nM)	K_{d1}/K_{d2}
WT	421.0 (203)	1.06	21	421.8 (216)	1.04	21	1.0
P2V	422.2 (202)	1.06	82	422.0 (219)	1.02	65	1.3
P2H	422.3 (180)	1.10	214	422.0 (216)	1.03	89	2.4
P2Y	422.6 (189)	1.09	108	422.0 (211)	1.05	40	2.7
ΔP3R4	422.8 (178)	1.14	242	422.3 (220)	1.01	33	7.3

[a] Samples were prepared as described under Experimental Procedures. [b] All peak positions are in nm; molar absorptivities assume a unique species and are in mM^{-1} cm^{-1}. [c] Ratio of intensities at $\lambda_\beta = 539$ nm, $\lambda_\alpha = 569$ nm. [d] Apparent binding affinity of Fe(II)-CO CooA protein samples for DNA as determined by an in vitro fluorescence polarization assay.

nm, were also present, confirming the presence of some high-spin ferrous heme. The MCD spectrum of Fe(II) ΔP3R4 displayed *C* terms having the greatest intensity among the variants, indicating ΔP3R4 had the highest proportion of high-spin ferrous heme (Figure 4B). The *C* terms in the variant spectra display a spectral pattern similar to that of high-spin Fe(II) myoglobin (Mb) (*52*) and the 5-coordinate, high-spin, CO-photolysis product of Fe(II) WT CooA (*22*). The close similarity between the positions of the high-spin MCD features of the N-terminal variants and the Fe(II) WT CO-photolysis product suggests that the high-spin heme of the variants may be 5-coordinate; however, both 5- and 6-coordinate high-spin hemes display similar MCD features (*52*), precluding unambiguous assignment of the coordination number for the high-spin component. The MCD spectral observations confirm the presence of variable amounts of high-spin ferrous heme in the N-terminal variants, and the intensity of the *C*-term MCD signals correlates with the apparent loss of intensity in the low-spin electronic absorption features of the variants.

DNA-Binding Affinity of the N-Terminal Variants Shows an Unexpected Dependence on the Order of CO Addition and Heme Reduction. The N-terminal CooA variants exhibit CO-dependent DNA binding, suggesting that alteration of the N terminus does not dramatically disrupt protein function. The in vitro DNA-binding activities of the Fe(III), Fe(II), and Fe(II)−CO states of all the N-terminal variants and WT CooA were measured; only the Fe(II)−CO forms bound to DNA (Table 2). Like WT CooA, the N-terminal variant CooA proteins failed to bind DNA in either the ferric or ferrous state (data not shown).

Surprisingly, the order of CO addition and heme reduction influenced the DNA-binding affinities of the N-terminal CooA variants. When N-terminal variants were incubated with CO after the heme was reduced (case 1), the DNA-binding affinities were weaker than if these same variants were incubated with CO before the heme was reduced (case 2) (Table 2). In contrast, the Fe(II)−CO form of WT CooA bound DNA with an affinity that was independent of the order of CO addition and reduction. In case 1, the DNA-binding affinities of the N-terminal variants were ∼4−10-fold weaker than that of WT CooA. Fe(II)−CO ΔP3R4 exhibited the poorest DNA-binding affinity among the variants, whereas Fe(II)−CO P2V exhibited the highest affinity. In case 2, the DNA-binding affinities of the N-terminal variants were enhanced compared to case 1 and were <4-fold weaker than that of WT CooA. The ratio of the DNA-binding affinities obtained according to the two methods (K_{d1}/K_{d2}) provides a measure of the sensitivity of a given variant to the order of CO addition and heme reduction (Table 2). The trend in these values suggests that protein response correlates with the extent to which the N-terminal length differs from that of WT CooA; the K_{d1}/K_{d2} ratio is largest for ΔP3R4 CooA and smallest for P2V CooA. In both cases 1 and 2, the DNA-binding affinities of P2H were comparatively lower than those of other variants, suggesting that the properties of P2H may be modestly different from those of the other variants (vide infra). The dependence of N-terminal variant DNA-binding affinities on the order of CO addition and reduction implies that there is a perturbation of the heme environment upon heme reduction that either alters WT-like CO binding or limits transmission of the CO signal.

Improved DNA binding was also observed when exogenous imidazole was added to the Fe(III) N-terminal variants prior to heme reduction and CO addition. Imidazole binds to the heme of Fe(III) ΔP3R4, converting the 5-coordinate, high-spin heme to fully 6-coordinate, low spin heme (*45*). When 25 mM imidazole was added to Fe(III) ΔP3R4, followed by sodium dithionite and then CO, the ΔP3R4 variant bound to DNA with an affinity similar to that of WT CooA (data not shown). However, if 25 mM imidazole was added to ΔP3R4 after sodium dithionite was added, subsequent incubation with CO resulted in only a slight enhancement of the DNA-binding affinity over a sample that did not contain imidazole. This imidazole effect was also observed for P2H and P2Y, but was modest and negligible for P2V and WT CooA, respectively (data not shown). That imidazole rescues case 1 DNA-binding affinity when added to the Fe(III) N-terminal variants suggests that there are perturbations in the ferric heme environments that influence the reduction process. It is plausible that the heme center defects are due to the 5-coordinate, high-spin heme present in the ferric state of the N-terminal variants because addition of an exogenous ligand restores native-like DNA-binding properties.

The Presence of a Distal Ligand in the Fe(III) State Is Apparently Required for Proper CooA Function: WT-like CO Binding to the Ferrous State That Enables DNA Binding. All N-terminal CooA variants incubated with CO after the heme is reduced (case 1) possess a different heme environment from when these same variants are incubated with CO before the heme is reduced (case 2). These differences are reflected in the relative intensities of the Soret, α, and β bands of the Fe(II)−CO adducts obtained according to the two methods (Table 2). As judged by molar absorptivities, case 1 CO-adducts displayed a Soret band with ∼10−20% less intensity than case 2 CO-adducts. The A_β/A_α intensity

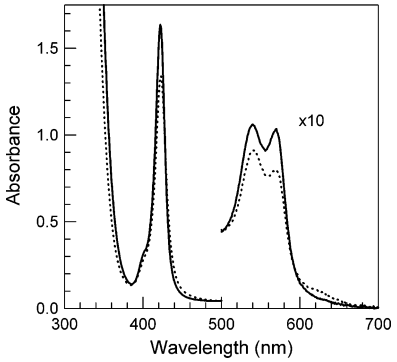

FIGURE 5: Electronic absorption spectra of Fe(II)−CO ΔP3R4 more closely resemble WT CooA when CO addition precedes reduction of the heme. Shown are optical spectra of Fe(II)−CO ΔP3R4 in 25 mM MOPS (pH 7.5) containing 0.1 M NaCl, which were formed by incubating a 7.0 μM CooA solution with CO either before (solid line) or after (dashed line) the addition of sodium dithionite (2 mM final concentration).

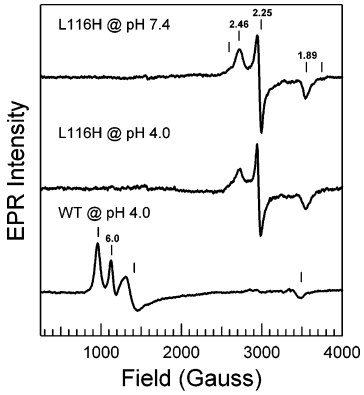

FIGURE 6: EPR spectroscopy strongly suggests His^{116} replaces Pro^2 as the distal heme ligand in Fe(III) L116H CooA. EPR samples were prepared either in 100 mM MOPS (pH 7.4) with 0.5 M NaCl or in 100 mM sodium acetate (pH 4.0) with 0.1 M NaCl. All EPR spectra were taken with a ~9.36-GHz microwave frequency, 100-kHz modulation frequency, and 8.3-G modulation amplitude. The spectrum of L116H CooA at pH 7.4 was the average of 16 scans and was recorded at 10 K, 0.505 mW of microwave power, and a 1.0×10^6 receiver gain. The spectrum of L116H CooA at pH 4.0 was the average of 32 scans and was recorded at 10 K, 0.127 mW of microwave power, and a receiver gain of 2.5×10^6. The spectrum of WT CooA was the average of 8 scans and was recorded at 4 K, 0.505 mW of microwave power, and a receiver gain of 5.0×10^5. Ferric $S = {}^1/_2$ heme was not observed in the EPR spectrum of WT CooA at pH 4.0 over a broad range of temperatures and powers (data not shown).

ratio among the N-terminal variants was also substantially greater and more unlike that of WT CooA in case 1 than in case 2. All N-terminal variants exhibited spectral features similar to those of Fe(II)−CO WT in case 2. In contrast, the spectral properties of the case 1 Fe(II)−CO adducts appear to relate to N-terminal length; variants with N termini most similar to that of WT CooA showed the greatest spectral similarity to Fe(II)−CO WT, whereas variants with dissimilar N termini showed the greatest spectral differences. For example, case 1 Fe(II)−CO ΔP3R4 displayed a spectrum least like that of WT CooA (Figure 5; Table 2). Despite the differences in intensity, the positions of the Soret, α, and β bands of all the CO-adducts, cases 1 and 2, are essentially identical. A large excess of CO induces no further spectral change in either case 1 or case 2, suggesting that the heme is fully CO bound in both cases. There is one distinct but weak feature at ~630 nm that appears in case 1 spectra but not in case 2; the identity of this band is unclear.

MCD spectroscopy confirms that CO binding to Fe(II) ΔP3R4 is essentially complete in both cases 1 and 2, but provides no further insight as to the nature of the differences in their heme environments. At 100 K, both case 1 and case 2 Fe(II)−CO ΔP3R4 adducts yielded MCD spectra that are typical of 6-coordinate, low-spin, CO-bound heme (Figure S3, Supporting Information), displaying principal *A* terms with crossovers at approximately 422 and 566 nm that occur near those reported for Fe(II)−CO WT CooA (*22*). Only slight differences between spectra of the case 1 and case 2 Fe(II)−CO ΔP3R4 samples were observed; a weak shoulder feature at ~554 nm was present in the MCD spectrum of the case 1 sample. This shoulder may indicate the presence of some unreacted 6-coordinate, low-spin, ferrous heme; however, the population of this species appears to be minimal on the basis of its low relative intensity. The similarities between the electronic absorption and MCD spectra of the case 1 and case 2 Fe(II)−CO adducts of ΔP3R4 do not necessarily imply that these two forms have identical heme coordination environments. Plausible abnormal structures, indistinguishable by the methods employed, include CO bound to the proximal (His^{77}) side of the heme or CO bound to the distal side of the heme in an altered local environment.

There is a direct correlation between DNA-binding affinity and the extent to which the spectral properties of the N-terminal variants are like those of Fe(II)−CO WT CooA (Table 2). Those variants for which the case 1 spectral properties are least like those of Fe(II)−CO WT are the same variants in which DNA-binding affinity is weakest. Additionally, variant CO adducts showing the greatest change in spectral properties between cases 1 and 2 also show the greatest change in DNA-binding affinity. For case 1 CO adducts, loss of DNA binding and loss of native spectral characteristics are most pronounced for ΔP3R4.

Replacement of the Weak Pro^2 Ligand by a Stronger Donor Is Likely Deleterious to CooA Function. A plausible explanation for the preferential binding of CO to the distal side of the CooA heme is that Pro^2 is a substantially weaker heme ligand than His^{77}. Although the crystal structure of Fe(II) CooA demonstrated that Pro^2 is buried within a hydrophobic pocket whereas the distal His^{77} ligand is solvent exposed (*18*), an NMR study by Aono provided definitive evidence that CO replaces Pro^2 upon binding (*23*). If the weak Pro^2 ligand is essential to protein function, the substitution of a stronger His ligand might prevent CO binding. Mutation of a leucine residue located in the distal heme pocket of CooA at position 116 has been shown to generate protein variants in which the 116 residue apparently replaces proline as a heme ligand (*31*). In this study, we have purified and characterized L116H CooA to determine whether substituting His^{116} as the distal ligand inhibits CO binding.

Spectroscopic characterization reveals that His^{116} likely replaces Pro^2 as the distal heme ligand in L116H CooA. The EPR spectrum of Fe(III) L116H at pH 7.4 is indicative of a thiolate-bound, 6-coordinate, low-spin heme, exhibiting a major set of rhombic EPR signals at $g = 2.46$, 2.25, and 1.89 and a minor set at $g = 2.59$, 2.25, and 1.84 (Figure 6). The positions of these signals are similar to those of Fe(III) WT CooA (Table S2, Supporting Information) (*21*). At pH 4.0, however, the EPR spectra of L116H and WT CooA are

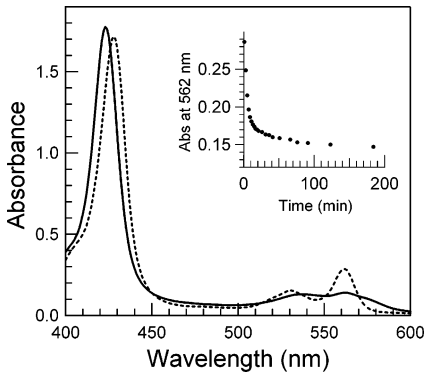

FIGURE 7: Formation of Fe(II)−CO L116H is much slower than the formation of WT CooA. The optical spectra of Fe(II) L116H (dashed line) and Fe(II)−CO L116H CooA (solid line) at $t = \sim 4$ h are shown. Both samples were ~6 μM in heme and were prepared in 25 mM MOPS (pH 7.5) containing 0.5 M NaCl. (Inset) Plot of absorbance at 562 nm versus time following CO addition suggests the reaction of CO with Fe(II)L116H approaches equilibrium.

substantially different (Figure 6). The EPR spectrum of L116H at pH 4.0 is similar to that at pH 7.4, revealing that the heme in L116H remains 6-coordinate and low-spin at low pH values. In contrast, the EPR spectrum of WT at pH 4.0 is characteristic of an exclusively high-spin ($S = {}^5/_2$) thiolate-ligated heme (Table S2, Supporting Information) (*45*). The observation that the heme of L116H is exclusively low-spin at pH 4.0 whereas the heme of WT CooA is high-spin reveals that WT CooA has a ligand that is more susceptible to protonation at pH 4.0, implying that His^{116} replaces Pro^2 as the distal ligand in L116H CooA. Electronic absorption spectra of L116H in both the Fe(III) and Fe(II) states provide further support that His^{116} replaces Pro^2 as the ligand. In Fe(III) L116H, the peak maxima of the Soret, β, and α bands occur at 425, 543, and 575 nm, whereas in the Fe(II) state the Soret, β, and α bands are present at 428, 530, and 562 nm, respectively. The positions of these spectral features are slightly shifted from those of WT CooA and are consistent with Cys/His coordination in the Fe(III) state (*34*−*36*) and His/His coordination in the Fe(II) state (*53*) of L116H CooA.

CO binding to Fe(II) L116H is substantially disrupted, further supporting the conclusion that the L116H heme is bound by the stronger His^{116} ligand. CO binding to Fe(II) L116H occurs more slowly than to Fe(II) WT CooA. For WT CooA, conversion of the Fe(II) species to the CO-bound adduct was rapid, with no change in the electronic absorption spectrum after initial mixing (data not shown). The N-terminal variants displayed behavior similar to that of WT CooA. For L116H, however, formation of the CO adduct occurred over an extended period of time and was easily followed (Figure 7). Conversion to Fe(II)−CO L116H was incomplete even after hours of reaction time; the α absorption band at 562 nm displayed noticeable intensity after 4 h, indicating that some Fe(II) L116H was still present. A plot of the loss of the 562 nm band with time (Figure 7, inset) suggested the reaction of CO with Fe(II) L116H approached equilibrium with 10−20% of the L116H protein remaining in the Fe(II) state (Figure 7). The MCD spectrum of the final product confirmed the presence of unreacted Fe(II) heme. No appreciable differences in the reaction between CO and Fe(II) L116H were observed when CO was added before or after the heme was reduced (data not shown). It should be noted that in this variant the identity of the ligand displaced by CO is not known; because His^{77} is solvent exposed in Fe(II) WT CooA, it is possible that His^{77} is more readily displaced by CO than the distal His^{116} ligand.

DISCUSSION

WT CooA and the N-Terminal Variants Utilize the N-Terminal Amino Group as the Distal Ligand in the Ferric State. Our characterization of the N-terminal CooA variants is consistent with N-terminal amine coordination in the ferric state, in which Pro^2 in WT and the N-terminal amino group in the N-terminal variants serve as the distal ligands. Previous spectroscopic and mutagenesis studies provided circumstantial evidence that Pro^2 served as the distal ligand in Fe(III) WT CooA (*17*, *20*−*22*, *30*, *54*). The best argument for Pro^2 ligation was articulated by Nakigima and co-workers (*30*): (1) a distal ligand other than Pro^2 in the Fe(III) state would require the unlikely displacement of both axial ligands upon reduction because Cys^{75} is replaced by His^{77} on the proximal side; (2) Fe(III) WT CooA does not bind exogenous ligands, suggesting that the distal heme ligand is an endogenous protein residue; and (3) only changes made to the N-terminal region alter the spectral characteristics of Fe(III) CooA, whereas mutagenesis of typical heme-binding residues had no effect. In the N-terminal variant proteins, the amount of abnormal 5-coordinate, high-spin heme is related to the difference between the length of the N terminus of the variant and that of WT CooA. This property is most striking when the Fe(III) P2V variant, with an N terminus the same length as that of WT CooA, is compared to variants with different N-terminal lengths, Fe(III) P2H, P2Y, and ΔP3R4. It is likely that the longer or shorter N terminus inhibits binding to the heme iron and that the 5-coordinate, high-spin, component in each variant arises from a population in which no distal ligand is bound. In P2V, there appears to be no potential endogenous sixth ligand other than the N-terminal amino group. In the longer P2H and P2Y variants, plausible alternate ligands include the Met^1 thioether (in either variant), His^2 (in P2H), and Tyr^2 (in P2Y).

A plausible alternative to N-terminal coordination in WT CooA and the N-terminal variants is that the N-terminal region poises a water molecule to bind the heme iron; however, this proposal is inconsistent with the observed pH-dependent behavior. All forms of CooA, WT and N-terminal variant, exhibited pH-dependent conversion from 6-coordinate, low-spin to 5-coordinate, high-spin hemes, with the 6-coordinate, low-spin species dominating at pH 10.0 and the 5-coordinate, high-spin species dominating at pH 3.0. The spectral characteristics of the high-spin and low-spin hemes were essentially the same for all Fe(III) CooA variants, suggesting that a common coordination structure was present. The conversion from low spin to high spin clearly occurs with loss of a heme ligand; MCD spectra of the low pH forms of WT CooA and the N-terminal variants are characteristic of cysteine-ligated 5-coordinate hemes. MCD spectra of camphor-free cytochrome P-450 (*51*) and Mb (*52*), in which water molecules serve as sixth ligands, are typical of 6-coordinate hemes, and only when the heme pocket becomes solvent inaccessible through substrate binding (P-450) or chemical modification (Mb) does the heme become 5-coordinate. If water were the sixth ligand in WT CooA and the N-terminal variants, this bound water would

undergo deprotonation at high pH, and by analogy to P450, the heme would be 6-coordinate at both high and low pH, bearing Cys^{75} and either hydroxide or water as the sixth ligand, respectively. This scenario is inconsistent with the observed coordination in the N-terminal variants. Because water is not present as a sixth ligand in the low-pH forms of CooA, the observed coordination and spin-state changes are most likely due to the proton-induced displacement of an endogenous protein-derived ligand. Loss of the distal ligand at low pH also rules out coordination by the thioether sulfur from Met^1 in the low-spin forms of Fe(III) P2H and Fe(III) P2Y as a thioether will not be protonated.

The observed pH dependence and spectral properties of Fe(III) WT CooA and the N-terminal variants are consistent with protonation displacing a weakly bound N-terminal amino group. The pH range over which loss of the distal ligand takes place varies with N-terminal length, suggesting that the distal ligand binding affinity varies in concert. WT Fe(III) CooA and P2V showed only minimal or modest pH-dependent spectral changes between pH 6.5 and 10.0, respectively; the conversion from 6-coordinate, low-spin to 5-coordinate, high-spin heme is virtually complete at pH 4.0. In contrast, Fe(III) P2H, P2Y (*29*), and ΔP3R4 displayed substantial spectral changes between pH 10.0 and 6.5, with nearly complete conversion from 6-coordinate, low spin to 5-coordinate, high spin occurring over this pH range. The more effective binding of protons to the distal ligand in P2H, P2Y, and ΔP3R4 suggests a substantial decrease in the affinity of the distal ligand for the heme iron in these variants. Because P2V behaves like WT CooA with respect to pH, the length of the N terminus appears to be a determinant of distal ligand affinity. Spectral characteristics provide further evidence for weak, N-terminal ligation. Comparison of the low-spin signals in EPR spectra of Fe(III) WT CooA and the N-terminal variants to Fe(III) cytochrome P-450 complexes with a range of exogenous ligands suggests that the distal heme ligand is neither an O-atom donor nor a "normal" N-atom donor like histidine but a weak N-atom donor (Table S2, Supporting Information) (*41*). The perturbation of spectral characteristics upon N-terminal modification of CooA in conjunction with the pH and length effects provide strong support for the conclusion that Pro^2 is the distal ligand in WT Fe(III) CooA and that the N-terminal amino group is the distal ligand in the Fe(III) N-terminal variants.

In certain N-terminal variants, a fraction of the protein population may contain heme in which the distal ligand is not the N terminus. For example, His^2 may be the distal ligand in a fraction of P2H molecules. Evidence in support of this suggestion includes the higher proportion of low-spin heme in Fe(III) P2H, relative to P2Y, and the poorer affinity of Fe(II)−CO P2H for DNA, which may result from an inability of CO to displace a strong His^2 ligand.

The Presence of a Weak N-Terminal Ligand in the Fe(III) State Enables CO-Dependent Activation of CooA: WT-like Reduction and CO Binding to the Ferrous State. The identity of the N-terminal amino acid is not critical for CooA function. Although the N-terminal variants contain different N-terminal amino acids, all of these variants are capable of CO-specific DNA binding. These results corroborate earlier in vivo data obtained by random mutagenesis (*29*) and agree with DNA-binding data reported for CooA variants with alterations at or near the N terminus and CooA homologues (*29*, *30*, *45*, *55*). In all of these studies, CO-dependent CooA function was retained despite modification of the N-terminal sequence. Because a variety of N-terminal amino acids support CO-dependent DNA binding by CooA, these results imply that CooA does not require a proline secondary amine as the distal ligand to function properly. That functional DNA binding and in vivo gene regulation are retained suggests that CO-dependent DNA binding by the N-terminal variants occurs by a mechanism similar to that of WT CooA.

The studies presented herein suggest that Pro^2 serves as the distal ligand in CooA because it is more weakly bound to heme than the proximal histidine ligand and, therefore, can be more readily displaced by CO. A weak ligand, such as an N-terminal amine, is important to enable distal CO binding to the CooA heme, as evidenced by the fact that CO binding is disrupted when the stronger His^{116} ligand replaces Pro^2 as the distal ligand in L116H CooA. Prior studies of CO binding to cytochrome b_5 demonstrated that the strength of the metal−ligand bond governs the ability of a low-spin 6-coordinate heme to bind CO (*56*, *57*). Cytochrome b_5, which contains a His^{39}/His^{63} coordinated heme, does not react appreciably with CO at higher pH values. At pH 3.5, however, cytochrome b_5 reacts with CO slowly and completely over ∼40 min (*57*). Formation of the Fe(II)−CO adduct at this low pH correlates with the onset of protein denaturation, which presumably weakens the Fe−His bond and facilitates ligand displacement. In contrast, a cytochrome b_5 H39M variant binds to CO at neutral pH, with CO coordinating the side of the heme with the Met^{39} residue (*56*). Together, these cytochrome b_5 studies imply that CO replaces an endogenous ligand only when that ligand is weakly bound to the heme iron.

CO-dependent activation requires that a distal ligand is present in the ferric state of CooA. For CO-dependent DNA binding, two processes must occur correctly: proximal ligand switching must occur upon reduction, and distal ligand displacement must occur upon CO binding. Abnormal DNA-binding activity in the N-terminal variants correlates with the amount of 5-coordinate, high-spin, ferric heme that is present, suggesting that the absence of a distal ligand in the Fe(III) state prevents WT-like CO binding to the Fe(II) state. In this context it is important to consider what the experimentally determined K_d values measure: each K_d value may be a weighted average of two variant CooA populations, one that binds DNA normally and one that fails to bind DNA. Alternatively, the measured K_d value may reflect a poorer affinity of the entire variant population. Four key observations from our spectroscopic and functional studies imply that the measured values are averages of two populations: (1) In the N-terminal variants, there are two populations of ferric heme that differ in their coordination, namely, 5-coordinate, high-spin and 6-coordinate, low-spin heme, and the amount of each coordination state varied with pH and N-terminal length. (2) When CO addition followed heme reduction, the measured K_d values and spectral properties of the CO-bound N-terminal variants depended on the length of the N terminus. (3) When CO addition preceded heme reduction, the DNA-binding affinities and absorption spectra of the N-terminal variants were comparable to those of WT CooA. Importantly, those variants with the largest amount of 5-coordinate, high-spin heme in the Fe(III) state showed the most substantial improvement in DNA binding (Table

2) when CO addition preceded reduction. (4) When the N-terminal variants were incubated with imidazole in the Fe(III) state prior to reduction and CO addition, DNA-binding activity could be rescued, suggesting that the presence of an exogenous distal ligand in the ferric state was sufficient to restore normal DNA binding. Together these observations suggest that *those N-terminal variant protein molecules without a distal ligand in the Fe(III) state do not undergo proper activation: neither reduction nor CO binding is like WT CooA, and therefore these protein molecules do not bind to DNA.*

We propose that the distal ligand anchors the heme cofactor during reduction, enabling proper CO and DNA binding. CooA undergoes a Cys^{75} to His^{77} ligand switch upon reduction (*17*, *20*, *22*); however, the crystal structure of Fe(II) CooA revealed a 4.8 Å separation between the Cys^{75} sulfur and the heme iron, implying that there must be substantial structural reorganization during ligand switching (*18*). We suggest that there is a significant perturbation of the distal heme pocket that occurs during the Cys^{75} to His^{77} ligand switch, which, in the absence of a distal heme ligand, leads to an inactive form of CooA. The key feature of this proposed mechanism is that the presence of a distal ligand in the Fe(III) state ultimately results in an active protein, whereas the absence of a distal heme ligand in the Fe(III) state leads to an inactive protein. We hypothesize that the distal heme pocket collapses upon heme reduction in the protein populations when the heme is 5-coordinate, high-spin, and that this collapse may either prevent CO binding on the distal side or alter CO binding in a way that does not allow for signal transmission. A mechanism involving a pocket collapse is supported by the observation that native-like function is restored when CO is added before the heme is reduced, suggesting that rapid CO binding rescues protein function. That the presence of CO during reduction rescues the protein suggests that CO binding occurs more rapidly than the inactivating pocket collapse. The pronounced improvement in DNA binding upon addition of imidazole to the Fe(III) state also supports this mechanism because the steric bulk created by an imidazole ligand would maintain the integrity of the distal heme pocket during ligand switching.

The spectroscopic and functional properties exhibited by all of the N-terminal variants (P2V, P2H, P2Y, and ΔP3R4) are qualitatively in good agreement with a pocket-collapse mechanism; however, the properties of P2H are modestly different. Although P2H and P2Y have the same N-terminal lengths, P2H has a larger amount of 6-coordinate, low-spin heme in both the ferric and ferrous states. On this basis, one might have expected that P2H would exhibit tighter DNA binding than P2Y; however, the DNA-binding affinity of P2H is weaker than that of P2Y. We interpret the differences between the properties of P2H and those of P2Y to arise because a fraction of P2H has His^2 as the distal ligand. The presence of a stronger sixth ligand in a fraction of the P2H protein would result in a low-spin heme that is resistant to CO activation.

The N-Terminal Proline Ligand Facilitates the CO-Specific Activation of CooA. Pro^2 facilitates the CO-specific activation of CooA by binding tightly enough to the heme to prevent adventitious ligand binding but weakly enough to be preferentially displaced by CO. Like other heme-sensory proteins, CooA requires effector-specific recognition (*3*). CooA enables its CO-specific response by (1) protecting the heme from adventitious ligand binding and (2) employing the weakly bound N-terminal ligand to ensure distal CO binding. To resist exogenous ligand binding, the heme in CooA is 6-coordinate, low-spin in the Fe(III), Fe(II), and Fe(II)−CO states; previous spectroscopic studies have shown that only the strongest ligands, NO or CO, bind to the WT CooA heme (*58*). Moreover, the N-terminal region of CooA further minimizes adventitious ligand binding by forming a solvent-inaccessible, hydrophobic pocket on the distal side of heme (*18*, *59*, *60*). To enable heme to function as a CO-specific sensor, the unique, weakly bound Pro^2 ligand is placed in this protected distal pocket. By employing a weak distal ligand on a 6-coordinate, low-spin heme, CooA is able to select for a strong exogenous ligand, namely, CO, and ensure that the distal ligand is replaced (*61*). Thus, utilization of the N-terminal Pro^2 as the unique distal ligand in CooA poises the protein for CO specificity.

ACKNOWLEDGMENT

We thank Dr. Marc Thorsteinsson for creating strains of the N-terminal variant proteins and Jose Serate for protein purification. We are grateful to Professor Thomas Brunold and his research group for assistance with, and use of, their MCD instrumentation. Finally, we thank Dr. Robert Kerby, Andrea Lee, and Sam Pazicni for helpful discussions and critical reading of the manuscript.

SUPPORTING INFORMATION AVAILABLE

Three figures showing (1) electronic absorption spectra of the Fe(III) forms of the N-terminal variants at pH 3.0 and 10.0, (2) the 25.0 K MCD spectrum of Fe(III) G117I CooA, and (3) MCD spectra of Fe(II)−CO ΔP3R4 formed by two methods; two tables containing electronic absorption and EPR spectral parameters of selected thiolate-ligated heme proteins and model complexes. This material is available free of charge via the Internet at http://pubs.acs.org.

REFERENCES

1. Rodgers, K. R. (1999) Heme-based sensors in biological systems, *Curr. Opin. Chem. Biol. 3*, 158−167.
2. Dioum, E. M., Rutter, J., Tuckerman, J. R., Gonzalez, G., Gilles-Gonzalez, M.-A., and McKnight, S. L. (2002) NPAS2: a gas-responsive transcription factor, *Science 298*, 2385−2387.
3. Jain, R., and Chan, M. K. (2003) Mechanisms of ligand discrimination by heme proteins, *J. Biol. Inorg. Chem. 8*, 1−11.
4. Park, H., Suquet, C., Satterlee, J. D., and Kang, C. (2004) Insights into signal transduction involving PAS domain oxygen-sensing heme proteins from the X-ray crystal structure of *Escherichia coli* Dos heme domain (*Ec* DosH), *Biochemistry 43*, 2738−2746.
5. Igarashi, J., Sato, A., Kitagawa, T., Yoshimura, T., Yamauchi, S., Sagami, I., and Shimizu, T. (2004) Activation of heme-regulated eukaryotic initiation factor 2α kinase by nitric oxide is induced by the formation of a five-coordinate NO-heme complex: optical absorption, electron spin resonance, and resonance Raman spectral studies, *J. Biol. Chem. 279*, 15752−15762.
6. Kurokawa, H., Lee, D.-S., Watanabe, M., Sagami, I., Mikami, B., Raman, C. S., and Shimizu, T. (2004) A redox-controlled molecular switch revealed by the crystal structure of a bacterial heme PAS sensor, *J. Biol. Chem. 279*, 20186−20193.
7. Stone, J. R., and Marletta, M. A. (1996) Spectral and kinetic studies on the activation of soluble guanylate cyclase by nitric oxide, *Biochemistry 35*, 1093−1099.
8. Dierks, E. A., Hu, S., Vogel, K. M., Yu, A. E., Spiro, T. G., and Burstyn, J. N. (1997) Demonstration of the role of scission of the proximal histidine-iron bond in the activation of soluble guanylyl

cyclase through metalloporphyrin substitution studies, *J. Am. Chem. Soc. 119*, 7316−7323.
9. Hobbs, A. J. (1997) Soluble guanylate cyclase: the forgotten sibling, *Trends Pharmacol. Sci. 18*, 484−491.
10. Gilles-Gonzalez, M. A., Ditta, G. S., and Helinski, D. R. (1991) A hemoprotein with kinase activity encoded by the oxygen sensor of *Rhizobium meliloti*, *Nature 350*, 170−172.
11. Gilles-Gonzalez, M. A., Gonzalez, G., and Perutz, M. F. (1995) Kinase activity of oxygen sensor FixL depends on the spin state of its heme iron, *Biochemistry 34*, 232−236.
12. He, Y., Shelver, D., Kerby, R. L., and Roberts, G. P. (1996) Characterization of a CO-responsive transcriptional activator from *Rhodospirillum rubrum*, *J. Biol. Chem. 271*, 120−123.
13. Shelver, D., Kerby, R. L., He, Y., and Roberts, G. P. (1997) CooA, a CO-sensing transcription factor from *Rhodospirillum rubrum*, is a CO-binding heme protein, *Proc. Natl. Acad. Sci. U.S.A. 94*, 11216−11220.
14. Kerby, R. L., Ludden, P. W., and Roberts, G. P. (1995) Carbon monoxide-dependent growth of *Rhodospirillum rubrum*, *J. Bacteriol. 177*, 2241−2244.
15. Aono, S., Nakajima, H., Saito, K., and Okada, M. (1996) A novel heme protein that acts as a carbon monoxide-dependent transcriptional activator in *Rhodospirillum rubrum*, *Biochem. Biophys. Res. Commun. 228*, 752−756.
16. Shelver, D., Kerby, R. L., He, Y., and Roberts, G. P. (1995) Carbon monoxide-induced activation of gene expression in *Rhodospirillum rubrum* requires the product of *cooA*, a member of the cyclic AMP receptor protein family of transcriptional regulators, *J. Bacteriol. 177*, 2157−2163.
17. Shelver, D., Thorsteinsson, M. V., Kerby, R. L., Chung, S.-Y., Roberts, G. P., Reynolds, M. F., Parks, R. B., and Burstyn, J. N. (1999) Identification of two important heme site residues (cysteine 75 and histidine 77) in CooA, the CO-sensing transcription factor of *Rhodospirillum rubrum*, *Biochemistry 38*, 2669−2678.
18. Lanzilotta, W. N., Schuller, D. J., Thorsteinsson, M. V., Kerby, R. L., Roberts, G. P., and Poulos, T. L. (2000) Structure of the CO sensing transcription activator CooA, *Nat. Struct. Biol. 7*, 876−880.
19. Kerby, R. L., Youn, H., Thorsteinsson, M. V., and Roberts, G. P. (2003) Repositioning about the dimer interface of the transcription regulator CooA: a major signal transduction pathway between the effector and DNA-binding domains, *J. Mol. Biol. 325*, 809−823.
20. Aono, S., Ohkubo, K., Matsuo, T., and Nakajima, H. (1998) Redox-controlled ligand exchange of the heme in the CO-sensing transcriptional activator CooA, *J. Biol. Chem. 273*, 25757−25764.
21. Reynolds, M. F., Shelver, D., Kerby, R. L., Parks, R. B., Roberts, G. P., and Burstyn, J. N. (1998) EPR and electronic absorption spectroscopies of the CO-sensing CooA protein reveal a cysteine-ligated low-spin ferric heme, *J. Am. Chem. Soc. 120*, 9080−9081.
22. Dhawan, I. K., Shelver, D., Thorsteinsson, M. V., Roberts, G. P., and Johnson, M. K. (1999) Probing the heme axial ligation in the CO-sensing CooA protein with magnetic circular dichroism spectroscopy, *Biochemistry 38*, 12805−12813.
23. Yamamoto, K., Ishikawa, H., Takahashi, S., Ishimori, K., Morishima, I., Nakajima, H., and Aono, S. (2001) Binding of CO at the Pro^2 side is crucial for the activation of CO-sensing transcriptional activator CooA. ^{1}H NMR spectroscopic studies, *J. Biol. Chem. 276*, 11473−11476.
24. Martinez, S. E., Huang, D., Szczepaniak, A., Cramer, W. A., and Smith, J. L. (1994) Crystal structure of chloroplast cytochrome *f* reveals a novel cytochrome fold and unexpected heme ligation, *Structure 2*, 95−105.
25. Martell, A. E., and Smith, R. M. (1974) *Critical Stability Constants*, p 37, Plenum Press, New York.
26. Radonovich, L. J., Bloom, A., and Hoard, J. L. (1972) Stereochemistry of low-spin iron porphyrins. II. Bis(piperidine)-α,*β*,*γ*,*δ*-tetraphenylporphinatoiron(II), *J. Am. Chem. Soc. 94*, 2073−2078.
27. Scheidt, W. R., Brinegar, A. C., Ferro, E. B., and Kirner, J. F. (1977) Nitrosylmetalloporphyrins. 4. Molecular stereochemistry of two crystalline forms of nitrosyl-α,*β*,*γ*,*δ*-tetraphenylporphinato-(4-methylpiperidine)iron(II). A structural correlation with *ν*(NO), *J. Am. Chem. Soc. 99*, 7315−7322.
28. Wyllie, G. R. A., Schulz, C. E., and Scheidt, W. R. (2003) Five- to six-coordination in (nitrosyl)iron(II) porphyrinates: effects of binding the sixth ligand, *Inorg. Chem. 42*, 5722−5734.
29. Thorsteinsson, M. V., Kerby, R. L., Conrad, M., Youn, H., Staples, C. R., Lanzilotta, W. N., Poulos, T. J., Serate, J., and Roberts, G. P. (2000) Characterization of variants altered at the N-terminal proline, a novel heme-axial ligand in CooA, the CO-sensing transcriptional activator, *J. Biol. Chem. 275*, 39332−39338.
30. Nakajima, H., Honma, Y., Tawara, T., Kato, T., Park, S. Y., Miyatake, H., Shiro, Y., and Aono, S. (2001) Redox properties and coordination structure of the heme in the CO-sensing transcriptional activator CooA, *J. Biol. Chem. 276*, 7055−7061.
31. Youn, H., Kerby, R. L., Thorsteinsson, M. V., Clark, R. W., Burstyn, J. N., and Roberts, G. P. (2002) Analysis of the L116K variant of CooA, the heme-containing CO sensor, suggests the presence of an unusual heme ligand resulting in novel activity, *J. Biol. Chem. 277*, 33616−33623.
32. Waterman, M. R. (1978) Spectral characterization of human hemoglobin and its derivatives, *Methods Enzymol. 52*, 456−463.
33. Lundblad, J. R., Laurance, M., and Goodman, R. H. (1996) Fluorescence polarization analysis of protein−DNA and protein−protein interactions, *Mol. Endocrinol. 10*, 607−612.
34. Lu, Y., Casimiro, D. R., Bren, K. L., Richards, J. H., and Gray, H. B. (1993) Structurally engineered cytochromes with unusual ligand-binding properties: expression of *Saccharomyces cerevisiae* Met-80→Ala iso-1-cytochrome *c*, *Proc. Natl. Acad. Sci. U.S.A. 90*, 11456−11459.
35. Sono, M., Dawson, J. H., Hall, K., and Hager, L. P. (1986) Ligand and halide binding properties of chloroperoxidase: peroxidase-type active site heme environment with cytochrome P-450 type endogenous axial ligand and spectroscopic properties, *Biochemistry 25*, 347−356.
36. Sigman, J. A., Pond, A. E., Dawson, J. H., and Lu, Y. (1999) Engineering cytochrome *c* peroxidase into cytochrome P450: a proximal effect on heme-thiolate ligation, *Biochemistry 38*, 11122−11129.
37. Yu, C. A., Gunsalus, I. C., Katagiri, M., Suhara, K., and Takemori, S. (1974) Cytochrome $P\text{-}450_{cam}$. I. Crystallization and properties, *J. Biol. Chem. 249*, 94−101.
38. Hollenberg, P. F., and Hager, L. P. (1973) The P-450 nature of the carbon monoxide complex of ferrous chloroperoxidase, *J. Biol. Chem. 248*, 2630−2633.
39. Roach, M. P., Pond, A. E., Thomas, M. R., Boxer, S. G., and Dawson, J. H. (1999) The role of the distal and proximal protein environments in controlling the ferric spin state and in stabilizing thiolate ligation in heme systems: thiolate adducts of the myoglobin H93G cavity mutant, *J. Am. Chem. Soc. 121*, 12088−12093.
40. Lipscomb, J. D. (1980) Electron paramagnetic resonance detectable states of cytochrome $P\text{-}450_{cam}$, *Biochemistry 19*, 3590−3599.
41. Dawson, J. H., Andersson, L. A., and Sono, M. (1982) Spectroscopic investigations of ferric cytochrome P-450-CAM ligand complexes. Identification of the ligand *trans* to cysteinate in the native enzyme, *J. Biol. Chem. 257*, 3606−3617.
42. Sono, M., Hager, L. P., and Dawson, J. H. (1991) Electron paramagnetic resonance investigations of exogenous ligand complexes of low-spin ferric chloroperoxidase: further support for endogenous thiolate ligation to the heme iron, *Biochim. Biophys. Acta 1078*, 351−359.
43. Wuttke, D. S. (1993) Preparation, characterization and intramolecular electron-transfer studies of ruthenium-modified cytochromes *c*, Ph.D. Thesis, pp 408−413, California Institute of Technology, Pasadena, CA.
44. Blumberg, W. E., and Peisach, J. (1971) Unified theory for low spin forms of all ferric heme proteins as studied by EPR, in *Probes and Structure and Function of Macromolecules and Membranes* (Chance, B., Yonetani, T., and Mildvan, A. S., Eds.) Vol. 2, pp 215−29, Academic Press, New York.
45. Youn, H., Kerby, R. L., Thorsteinsson, M. V., Conrad, M., Staples, C. R., Serate, J., Beack, J., and Roberts, G. P. (2001) The heme pocket afforded by Gly^{117} is crucial for proper heme ligation and activity of CooA, *J. Biol. Chem. 276*, 41603−41610.
46. Hollenberg, P. F., Hager, L. P., Blumberg, W. E., and Peisach, J. (1980) An electron paramagnetic resonance study of the high and low spin forms of chloroperoxidase, *J. Biol. Chem. 255*, 4801−4807.
47. Tsai, A.-L., Berka, V., Chen, P.-F., and Palmer, G. (1996) Characterization of endothelial nitric-oxide synthase and its reaction with ligand by electron paramagnetic resonance, *J. Biol. Chem. 271*, 32563−32571.
48. Tang, S. C., Koch, S., Papaefthymiou, G. C., Foner, S., Frankel, R. B., Ibers, J. A., and Holm, R. H. (1976) Axial ligation modes in iron(III) porphyrins. Models for the oxidized reaction states of cytochrome P-450 enzymes and the molecular structure of iron-

(III) protoporphyrin IX dimethyl ester *p*-nitrobenzenethiolate, *J. Am. Chem. Soc. 98*, 2414−2434.
49. Dawson, J. H., Trudell, J. R., Barth, G., Linder, R. E., Bunnenberg, E., Djerassi, C., Chiang, R., and Hager, L. P. (1976) Chloroperoxidase. Evidence for P-450 type heme environment from magnetic circular dichroism spectroscopy, *J. Am. Chem. Soc. 98*, 3709−3710.
50. Sono, M., Stuehr, D. J., Ikeda-Saito, M., and Dawson, J. H. (1995) Identification of nitric oxide synthase as a thiolate-ligated heme protein using magnetic circular dichroism spectroscopy. Comparison with cytochrome P-450-CAM and chloroperoxidase, *J. Biol. Chem. 270*, 19943−19948.
51. Vickery, L., Salmon, A., and Sauer, K. (1975) Magnetic circular dichroism studies on microsomal aryl hydrocarbon hydroxylase. Comparison with cytochrome b_5 and cytochrome $P450_{cam}$, *Biochim. Biophys. Acta 386*, 87−98.
52. Bracete, A. M., Sono, M., and Dawson, J. H. (1991) Effects of cyanogen bromide modification of the distal histidine on the spectroscopic and ligand binding properties of myoglobin: magnetic circular dichroism spectroscopy as a probe of distal water ligation in ferric high-spin histidine-bound heme proteins, *Biochim. Biophys. Acta 1080*, 264−270.
53. Sawai, H., Kawada, N., Yoshizato, K., Nakajima, H., Aono, S., and Shiro, Y. (2003) Characterization of the heme environmental structure of cytoglobin, a fourth globin in humans, *Biochemistry 42*, 5133−5142.
54. Yamashita, T., Hoashi, Y., Watanabe, K., Tomisugi, Y., Ishikawa, Y., and Uno, T. (2004) Roles of heme axial ligands in the regulation of CO binding to CooA, *J. Biol. Chem. 279*, 21394−21400.
55. Youn, H., Kerby, R. L., Conrad, M., and Roberts, G. P. (2004) Functionally critical elements of CooA-related CO sensors, *J. Bacteriol. 186*, 1320−1329.
56. Sligar, S. G., Egeberg, K. D., Sage, J. T., Morikis, D., and Champion, P. M. (1987) Alteration of heme axial ligands by site-directed mutagenesis: a cytochrome becomes a catalytic demethylase, *J. Am. Chem. Soc. 109*, 7896−7897.
57. Hirota, S., Kishi, M., Yamauchi, O., Wang, Y.-H., and Huang, Z.-X. (2001) Carbon monoxide complex of cytochrome b_5 at acidic pH, *Biochem. Biophys. Res. Commun. 282*, 351−355.
58. Reynolds, M. F., Parks, R. B., Burstyn, J. N., Shelver, D., Thorsteinsson, M. V., Kerby, R. L., Roberts, G. P., Vogel, K. M., and Spiro, T. G. (2000) Electronic absorption, EPR, and resonance Raman spectroscopy of CooA, a CO-sensing transcription activator from *R. rubrum*, reveals a five-coordinate NO-heme, *Biochemistry 39*, 388−396.
59. Youn, H., Kerby Robert, L., and Roberts, G. P. (2003) The role of the hydrophobic distal heme pocket of CooA in ligand sensing and response, *J. Biol. Chem. 278*, 2333−2340.
60. Coyle, C. M., Puranik, M., Youn, H., Nielsen, S. B., Williams, R. D., Kerby, R. L., Roberts, G. P., and Spiro, T. G. (2003) Activation mechanism of the CO sensor CooA: mutational and resonance Raman spectroscopic studies, *J. Biol. Chem. 278*, 35384−35393.
61. Puranik, M., Nielsen, S. B., Youn, H., Hvitved, A. N., Bourassa, J. L., Case, M. A., Tengroth, C., Balakrishnan, G., Thorsteinsson, M. V., Groves, J. T., McLendon, G. L., Roberts, G. P., Olson, J. S., and Spiro, T. G. (2004) Dynamics of carbon monoxide binding to CooA, *J. Biol. Chem. 279*, 21096−21108.

BI0487948